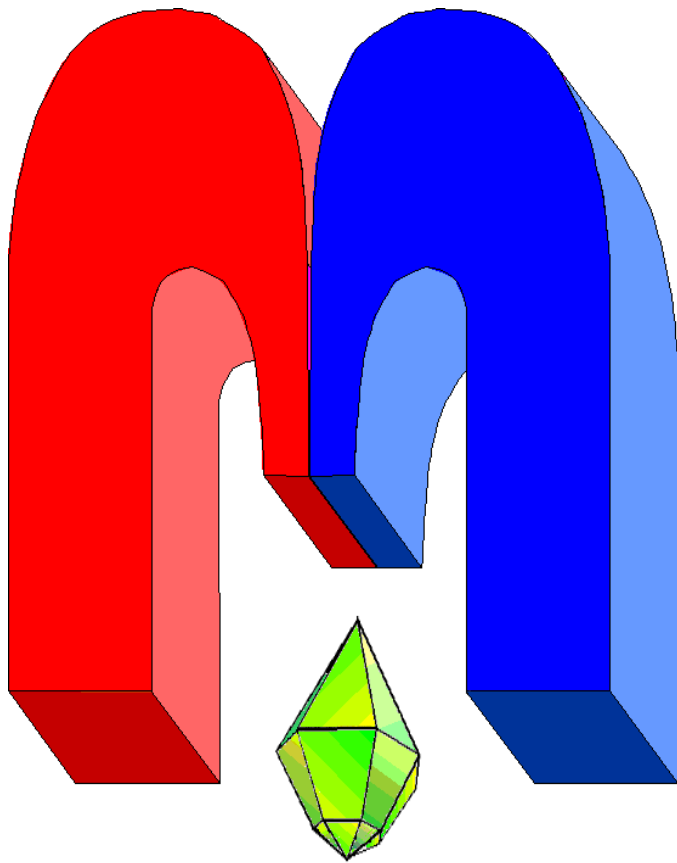


ISSN 2072-5981

doi: 10.26907/mrsej



***magnetic
Resonance
in Solids***

Electronic Journal

Volume 25

Issue 1

Article No 23102

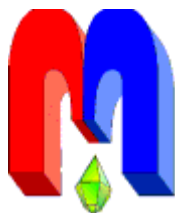
1-8 pages

2023

doi: [10.26907/mrsej-23102](https://doi.org/10.26907/mrsej-23102)

<http://mrsej.kpfu.ru>

<http://mrsej.ksu.ru>



Established and published by Kazan University*
Endorsed by International Society of Magnetic Resonance (ISMAR)
Registered by Russian Federation Committee on Press (#015140),
August 2, 1996
First Issue appeared on July 25, 1997

© Kazan Federal University (KFU)†

"Magnetic Resonance in Solids. Electronic Journal" (MRSej) is a peer-reviewed, all electronic journal, publishing articles which meet the highest standards of scientific quality in the field of basic research of a magnetic resonance in solids and related phenomena.

Indexed and abstracted by
*Web of Science (ESCI, Clarivate Analytics, from 2015),
Scopus (Elsevier, from 2012), RusIndexSC (eLibrary, from 2006), Google Scholar,
DOAJ, ROAD, CyberLeninka (from 2006), SCImago Journal & Country Rank, etc.*

Editor-in-Chief

Boris **Kochelaev** (KFU, Kazan)

Honorary Editors

Jean **Jeener** (Universite Libre de Bruxelles, Brussels)

Raymond **Orbach** (University of California, Riverside)

Executive Editor

Yurii **Proshin** (KFU, Kazan)
mrsej@kpfu.ru



This work is licensed under a [Creative Commons Attribution-ShareAlike 4.0 International License](https://creativecommons.org/licenses/by-sa/4.0/).

 This is an open access journal which means that all content is freely available without charge to the user or his/her institution. This is in accordance with the [BOAI definition of open access](https://www.boai.ru/).

Technical Editor

Maxim **Avdeev** (KFU, Kazan)

Editors

Vadim **Atsarkin** (Institute of Radio Engineering and Electronics, Moscow)

Yurij **Bunkov** (CNRS, Grenoble)

Mikhail **Eremin** (KFU, Kazan)

David **Fushman** (University of Maryland, College Park)

Hugo **Keller** (University of Zürich, Zürich)

Yoshio **Kitaoka** (Osaka University, Osaka)

Boris **Malkin** (KFU, Kazan)

Alexander **Shengelaya** (Tbilisi State University, Tbilisi)

Jörg **Sichelschmidt** (Max Planck Institute for Chemical Physics of Solids, Dresden)

Haruhiko **Suzuki** (Kanazawa University, Kanazava)

Murat **Tagirov** (KFU, Kazan)

Dmitrii **Tayurskii** (KFU, Kazan)

Valentine **Zhikharev** (KNRTU, Kazan)

* Address: "Magnetic Resonance in Solids. Electronic Journal", Kazan Federal University; Kremlevskaya str., 18; Kazan 420008, Russia

† In Kazan University the Electron Paramagnetic Resonance (EPR) was discovered by Zavoisky E.K. in 1944.

Magnetic resonance studies of Ar-ion irradiated rutile

A.A. Sukhanov*, V.F. Valeev, V.I. Nuzhdin, R.I. Khaibullin

Zavoisky Physical-Technical Institute,
FRC Kazan Scientific Center of RAS, Kazan 420029, Russia

**E-mail: ansukhanov@mail.ru*

(received November 28, 2022; revised February 21, 2023; accepted December 14, 2022;

published February 26, 2023)

The point defects have been produced in the rutile structure by irradiation of a single crystalline (001)-TiO₂ rutile platet wih 40 keV Ar⁺ ions. It is found that Ar-ion bombardment of rutile results in a large number of positively charged oxygen vacancies and, as a consequence, leads to a change in the valence of neighbouring Ti cations. Electron paramagnetic resonance (EPR) of Ar-ion irradiated TiO₂ rutile is studied in detail. The analysis of angular and temperature dependences of EPR spectra makes it possible to conclude that EPR signals are associated with Ti³⁺ ions in the sixfold symmetric environment. In addition to the main signal from even titanium isotopes, eight equidistant weak lines are observed due to the hyperfine interaction typical for two titanium isotopes: ⁴⁷Ti with a nuclear spin $I = 5/2$ (natural abundance of 7.4%) and ⁴⁹Ti with a nuclear spin $I = 7/2$ (natural abundance of 5.4%). By comparing the g -tensor components with the reference data it is concluded that these Ti³⁺-based centers in Ar-ion implanted rutile were not described before.

PACS: 61.72.Hh, 61.72.Ji, 68.55.Ln

Keywords: electron paramagnetic resonance, rutile, ion implantation, oxygen vacancies, Ti³⁺ ions, g -factors

1. Introduction

Titanium dioxide (TiO₂) is one of the well-studied metal oxides due to its many interesting applications. TiO₂ is widely used in heterogeneous catalysis as a photocatalyst, in solar cells, gas sensor; as white pigment in paints and cosmetic products; as a corrosion-protective, energy-saving and self-cleaning optical coating; and in electric devices such as varistors [1,2]. Moreover, as a material revealing the memristive effect [3], TiO₂ has recently found wide application prospects for artificial biological systems and non-volatile random access memory [4]. Note that the technological importance of TiO₂ is inseparably related to various types of defects such as oxygen vacancies (V_O), Ti³⁺ ions on regular lattice sites, Ti interstitials, crystallographic shear planes, as well as substitutional impurity atoms introduced by doping into TiO₂. Titanium dioxide crystallizes in three different polymorphic modifications: rutile, anatase, and brookite [1, 5]. Rutile is the most thermodynamically stable crystalline state of TiO₂. Rutile has a tetragonal crystal structure (lattice parameters are $a = b = 0.465$ nm and $c = 0.297$ nm), in which each Ti ion is surrounded by an octahedron of O ions, as it is shown in Fig. 1. The stoichiometric rutile, TiO₂, is an insulator with a band gap of 3 eV, transparent in the visible wavelength range, and a diamagnet. It transforms into oxygen-deficient nonstoichiometric rutile TiO_{2-x}, where x is usually between 10⁻⁴ and 10⁻², under high-temperature annealing in a reducing atmosphere (e.g., in vacuum) or after heavily electron irradiation [1]. The oxygen-deficient reduced rutile is an n-type semiconductor [5] and a paramagnet [6] due to the point defects such as oxygen vacancies and paramagnetic Ti³⁺ ions in the rutile structure. Moreover, the reduction of rutile under heating in ultra-high vacuum leads to visible color changes from colorless to light blue and, eventually, dark blue hues depending on the level of the oxygen loss (x), hence on the concentration of oxygen vacancies [1, 5, 6]. It is important to note that an oxygen vacancy

has an effective charge of +2. They can act as electron traps and have different charge states varying from doubly ionized unoccupied (V_O^{++}) to singly ionized V_O^+ or even neutral V_O^0 states, respectively, by trapping one or two electrons.

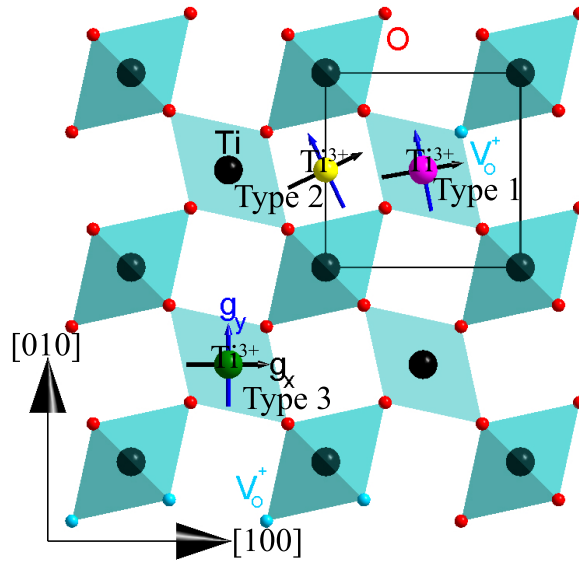


Figure 1. Polyhedral model of the rutile crystal viewed along the [001] axis. Three different types of Ti^{3+} point defects in the rutile lattice are shown schematically by principal axes of the g -factor tensor taken from Table 1.

Earlier near-stoichiometric and TiO_{2-x} rutile crystals have been intensively studied by electron paramagnetic resonance (EPR) [7–11]. The paramagnetic species of different origins were found in the rutile crystals in the magnetic field region of 320–400 mT in the X-band. All these centers can be divided into three large groups associated with either Ti^{3+} ions or oxygen vacancies, or with the uncontrolled contamination of rutile samples by paramagnetic impurities, e.g., 3d ions. EPR reveals a structural Ti^{3+} ion surrounded by an octahedron of five oxygen atoms with a positively charged oxygen vacancy (Type 1 in Fig. 1) and a Ti^{3+} ion located in the interstitial position (Type 2). They are typical Ti-based paramagnetic centers in slightly reduced TiO_2 samples [7–10]. However, the concentration of these paramagnetic Ti centers decreases fast when the oxygen deficiency in rutile increases [7]. Dark blue rutile crystals with higher concentrations of oxygen vacancies are EPR-silent and exhibit extended Ti^{3+} -related bulk defects such as crystallographic shear planes (not shown in Fig. 1). EPR spectra from singly ionized V_O^+ with $S = 1/2$ and neutral V_O^0 oxygen vacancies with $S = 1$ were observed in stoichiometric or slightly reduced TiO_2 samples [9, 10]. The centers with g -factors close to the free electron g -factor of 2.00232 were observed only at low temperature (35 K) and under photo-irradiation with a wavelength close to the band gap.

In this work, we used intense irradiation with high-energy Ar^+ ions to generate a large number of radiation defects (oxygen vacancies, Ti interstitials etc.) in the surface TiO_2 layer. According to SRIM (Stopping and Range of Ions in Matter) calculations [12], the concentration of point defects in the irradiated oxide layer can reach colossal values on the order of 10^{22} cm^{-3} . In other words, there was no need to create oxygen vacancies in TiO_2 rutile using traditional methods such as high-temperature annealing in vacuum. Moreover, we developed an original method of migration of oxygen vacancies under an applied DC electric field (electromigration procedure) in order to change the concentration of these point defects in the sample. We used EPR to characterize paramagnetic centers in Ar-ion irradiated rutile.

2. Experimental details

The single-crystal (001) face-oriented TiO_2 plates of synthetic rutile (Moscow Power Engineering Institute, Lab. of Prof. A. Balbashov) were irradiated with 40 keV Ar^+ ions on an ILU-3 ion-beam accelerator (ZPTI, FRC Kazan Scientific Center of RAS) at an elevated substrate temperature of 900 K during ion irradiation. The ion irradiation was carried out to the fluency of 1.5×10^{17} ion/cm² at an ion current density of $8 \mu\text{A}/\text{cm}^2$. It is seen clearly in Fig. 2 that initially colorless TiO_2 plates (a) acquire a sky-blue hue (b) due to the formation of oxygen vacancies in the surface region (of about 100 nm thickness [12]) of Ar-ion irradiated TiO_2 rutile.

The chemical element microanalysis using a Carl Zeiss EVO 50 XVP scanning electron microscope equipped with an Oxford Inca Energy-350 EDS spectrometer confirmed the formation of oxygen vacancies in Ar-ion implanted rutile. The oxygen concentration in the irradiated sample is reduced by about 3–4 at.% in comparison with the oxygen concentration in the virgin rutile plate (66–67 at.%). No argon was detected in the irradiated sample. Chemically inert argon does not form chemical bonds with rutile, and after ion irradiation, argon leaves the irradiated region of rutile due to outward diffusion.

Fast radiation-enhanced electromigration of positively charged oxygen vacancies become visually observable when the voltage (15 V) is supplied to sample under study. As it is shown in Fig. 2c, after applying the electromigration procedure, the initial sky-blue color of the samples changed into the dark blue-grey around the negative electrode, while the region around the positive electrode lost its coloration due to a decrease in the concentration of oxygen vacancies in this part of a sample.

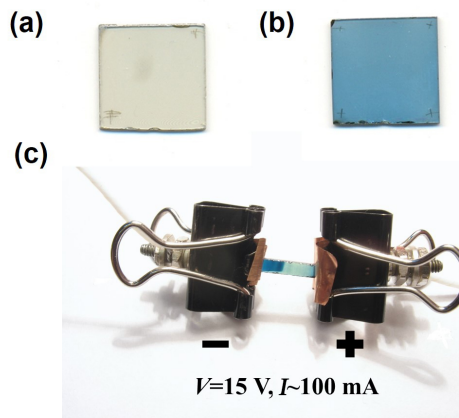


Figure 2. Photos of experimental samples: a) virgin rutile TiO_2 plate; b) TiO_2 plate irradiated with 40 keV Ar^+ ions to a fluency of 1.5×10^{17} ion/cm²; c) Ar-ion irradiated TiO_2 strip with sizes of $10 \times 2 \times 1.5 \text{ mm}^3$ after electromigration of positively charged oxygen vacancies to the negative electrode.

Three samples with different concentration of oxygen vacancies were used in EPR measurements: as-irradiated, dark blue-grey and light blue ones. The dark blue-grey and light blue samples were prepared by cutting the strip (see Fig. 2c) near the negative and positive electrodes, respectively, after the electromigration procedure. All samples had the form of rectangular parallelepipeds with the sizes of $2 \times 2 \times 1.5 \text{ mm}^3$. The angular dependence of the EPR spectra was measured on a Bruker ELEXSYS E580 EPR spectrometer with an ER4116DM resonator in the X-band (9.65 GHz) at a temperature of 30 K using an E218-1001 programmable goniometer. The accuracy of setting the rotation angle was ± 0.5 degrees. The angular dependence of the

EPR spectra was measured in three orthogonal (001), (100) and (010) planes of the sample. The temperature dependence of the spectra was measured in the temperature range from 5 to 100 K using an Oxford flow cryostat ESR 900. Moreover, the light-stimulated EPR experiment was carried out at a temperature of 30 K by using a diode laser with a wavelength of 430 nm and a power of 10 mW.

3. Results

Figure 3 shows the experimental EPR spectra of the as-irradiated sample at an applied magnetic field \mathbf{B} directed parallel to the [100] axis of rutile. Figure 3 shows that one signal is observed above 60 K. This signal is marked as a background signal because it was also observed in the virgin TiO_2 plate before the irradiation with argon ions. Although the background signal has some angular dependence and moves towards saturation in lower temperatures of 5–20 K, we exclude it from further consideration, since it is associated with uncontrolled contamination of the sample. It is important to note that a new signal with an anisotropic g factor appears in rutile samples irradiated with Ar ions. This signal is marked as the main one in the EPR spectra shown in Fig. 3, since its behavior depends on the concentration of oxygen vacancies in the sample. Namely, in a light blue sample with a reduced concentration of oxygen vacancies, the intensity of this signal is much lower compared to that of the initially as-irradiated sample. On the contrary, this signal completely disappears in the dark blue-gray sample with the highest concentration of oxygen vacancies.

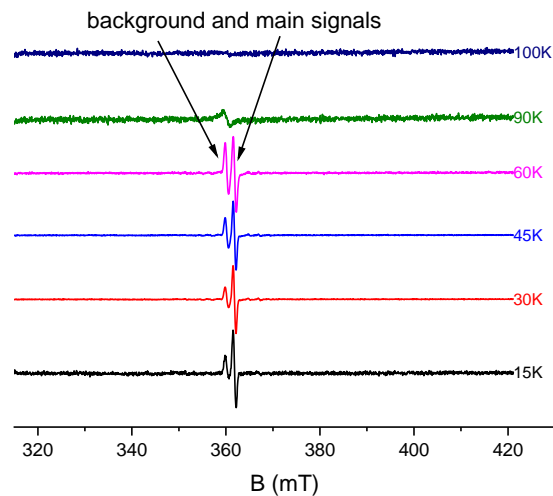


Figure 3. Temperature dependence of EPR spectra of Ar-ion irradiated TiO_2 sample for magnetic field \mathbf{B} parallel to the [100] axis. For better visibility, the amplitude of main signal in the spectra taken at temperatures below 60 K was normalized to unity.

In order to establish the origin of the main signal, namely, the structural position and local symmetry of the paramagnetic center associated with this signal, the angular dependences of the EPR spectra of as-irradiated sample in various crystallographic planes of rutile were studied in detail. Figure 4a shows the angular dependence for the (001) plane, the analysis of which indicates the presence of two magnetically nonequivalent centers in the as-irradiated sample. Figure 4b shows the angular dependences of the EPR spectra for the (010) plane. In this case, one center is observed. Note that a very similar angular dependence of EPR spectra was also observed at the rotation of magnetic field \mathbf{B} in equivalent the (100) plane of rutile (not shown). As follows from the analysis of angular dependences shown in Fig. 4, the EPR lines from two

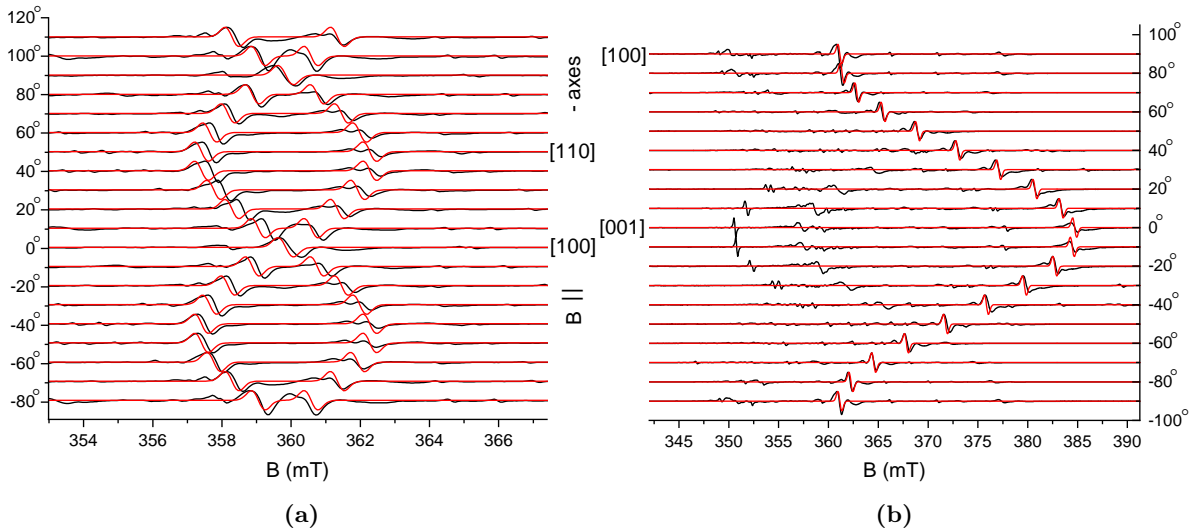


Figure 4. Angular dependences of EPR spectra of the Ar-ion irradiated TiO_2 sample at the rotation of magnetic field \mathbf{B} in the (001) plane (a) and in the (010) plane (b) at 30 K. Black and red lines show experimental data and the simulation results, respectively.

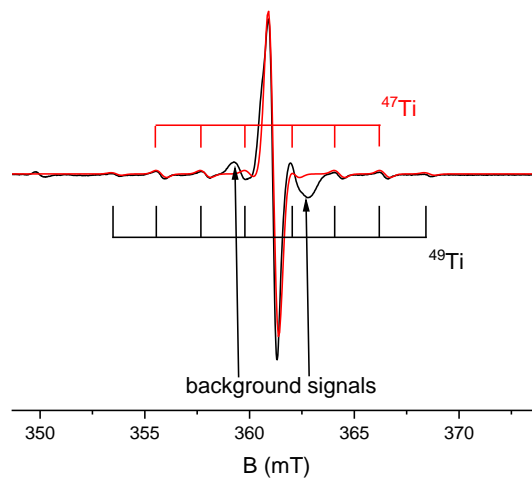


Figure 5. EPR spectrum of the Ar-ion irradiated TiO_2 sample for magnetic field \mathbf{B} is parallel to the [100] axis at 30 K. Black and red lines show experimental data and the simulation results, respectively. The hyperfine splitting of the simulated spectrum is 57 MHz. Two signals around the central EPR line are the background signals and not hyperfine splitting components of the central line.

magnetically nonequivalent centers coincide with each other when the magnetic field is directed along the [100] axis or \mathbf{B} rotates in the (010) plane. In this case, the spectrum (Fig. 5) taken at a small sweep of the magnetic field reveals weak lines due to the hyperfine interaction with nuclear spins associated with two titanium isotopes: ^{47}Ti and ^{49}Ti with a natural abundance of 7.4% and 5.4%, respectively. The ^{47}Ti isotope has a nuclear spin $I = 5/2$, and six lines are to be observed in the spectrum, and the ^{49}Ti isotope has $I = 7/2$, in this case, there are eight lines in the spectrum. At the natural isotopic abundance, the sum of two spectra with different hyperfine structures and of low intensity is observed, and the intensity of the most extreme lines in the hyperfine structure is less.

The observed EPR spectra were described in the spin-Hamiltonian model:

$$H = \beta \mathbf{S} \mathbf{g} \mathbf{B},$$

where $S = 1/2$, β is a Bohr magneton, \mathbf{g} is g -tensor, \mathbf{B} is a magnetic field. The hyperfine interaction was not taken into account to describe the angular dependence of the EPR spectra. The EPR spectra were calculated using the EasySpin software toolbox [13]. The g -tensor values for the principal axes were determined from the calculation of all observed angular dependences for both the as-irradiated rutile sample and light blue sample with lower concentration of oxygen vacancies, and are given in Table 1. Note that previously observed EPR spectra of Ti^{3+} in reduced rutile (similar to those for the light blue sample) were observed only under photo-irradiation [9,10]. We observed a signal in as-irradiated and light blue samples without photo-irradiation, and no effect of photo-irradiation on the observed EPR signal was found.

Table 1. Principal values and principal axes of the g -tensor for three types of the Ti^{3+} ions. The positions of these different Ti^{3+} ions in the rutile lattice are shown in Fig. 1.

| Principal value | Principal-axis direction | Type of the position in the rutile lattice | References |
|--|---|--|------------|
| $g_1 = 1.9572$ $g_2 = 1.9187$ $g_3 = 1.8239$ | $[100] \pm 3.1^\circ$ $[010] \pm 3.1^\circ$ $[001]$ | structural, Type 1 | [10] |
| $g_1 = 1.9526$ $g_2 = 1.9117$ $g_3 = 1.8132$ | $[100] \pm 4^\circ$ $[010] \pm 4^\circ$ $[00\bar{1}]$ | structural, Type 1 | [9] |
| $g_1 = 1.9746$ $g_2 = 1.9780$ $g_3 = 1.9414$ | $[100] \pm 26^\circ$ $[010] \pm 26^\circ$ $[001]$ | interstitial, Type 2 | [7] |
| $g_1 = 1.9766$ $g_2 = 1.9738$ $g_3 = 1.9408$ | not defined | structural | [11] |
| $g_x = 1.922$ $g_y = 1.896$ $g_z = 1.791$ | $[100]$ $[010]$ $[001]$ | structural, Type 3 | this work |

4. Discussion

Based on the observation of hyperfine splitting in the EPR spectrum (Figure 5), it can be argued that this spectrum is associated with paramagnetic Ti^{3+} ions. EPR of Ti^{3+} ions in oxygen-deficient non-stoichiometric TiO_{2-x} rutile was previously observed and discussed within the structural model, where the substitutional Ti^{3+} ions are accompanied by the nearest oxygen vacancies forming the defect $\text{Ti}^{3+}\text{-V}_\text{O}^+$ complexes [8,10,11]. The EPR spectra of these substitutional Ti^{3+} ions were observed at temperatures below 30 K and under photo-irradiation only. Another possibility is to observe EPR spectra from Ti^{3+} ions in rutile for the interstitial position of Ti^{3+} . However, for the interstitial position of Ti^{3+} ions, the fourfold splitting of the Ti^{3+} EPR lines is usually observed when the magnetic field orientation varies from the $[001]$ axis to the $[110]$ axis [7]. In our case, there is the twofold splitting of the Ti^{3+} EPR lines in the (001) plane, which is characteristic of the substitution of Ti^{3+} ions in rutile. The simulation of the

angular dependences of the EPR spectra convincingly indicates that the Ti^{3+} ion is in the structural position of the rutile lattice. In the rutile lattice, Ti ions are surrounded by an octahedron of six oxygen atoms. In this case, the titanium ion should have the Ti^{4+} valence state. The large number of positively charged oxygen vacancies in a sample irradiated with Ar ions can lead to a decrease in the titanium valence due to nonlocal charge compensation. In our case, the EPR spectrum is observed at low temperatures, the same as in the cases mentioned above for oxygen-deficient rutile TiO_{2-x} [8, 9], but without photo-irradiation. From the simulation of the EPR spectra, it was found that the principal values of g -factors along the equivalent [100]- and [010]-crystallographic axes are slightly different. This difference can be explained either by the Jahn-Teller effect [14] or by mechanical stresses in the rutile plates after intense ion irradiation [12]. Each of these processes leads to a slight distortion of the local structure and a decrease in the local symmetry of the Ti^{3+} ions from tetragonal to rhombic one. For the blue sample with a low concentration of oxygen vacancies, the local environment of the Ti^{3+} ion did not change, and the EPR spectrum is very similar to the EPR spectrum of the as-irradiated sample. The high concentration of oxygen vacancies in the dark blue-gray sample leads to an increase in the concentration of Ti^{3+} ions and the formation of antiferromagnetic exchange-coupled pairs Ti^{3+} - Ti^{3+} [15, 16]. In this case, the EPR spectrum would not be observed.

5. Summary

Summarizing the obtained results, we can conclude the following. The intense irradiation of rutile, TiO_2 , with high-energy Ar^+ ions results in the coloration of crystals in blue hues and the formation of a large number of positively charged oxygen vacancies in the rutile structure. The concentration of oxygen vacancies in a given spatial region of the irradiated rutile is easily controlled using the applied electric field (electromigration procedure). A new paramagnetic center associated with Ti^{3+} ions is found in TiO_2 rutile heavily irradiated with Ar ions. The principal values of the g -tensor and the directions of the principal axes of the g -tensor of this center have not been reported before. We proposed a structural model of this center, in which paramagnetic Ti^{3+} ions occupy lattice sites surrounded by an octahedron of six oxygen anions. The high concentration of positively charged oxygen vacancies in the irradiated region of rutile ensures the charge neutrality of the TiO_2 crystal and the thermodynamic stability of these EPR active Ti^{3+} ions in the rutile lattice. Finally, unlike the earlier published data, we observed the EPR spectra of Ti^{3+} ions located in lattice sites of rutile without photo-irradiation of the sample under study. Moreover, there was no any effect of additional photo-irradiation on the intensity and linewidth of the observed EPR signal.

Acknowledgments

The study was supported by the Russian Science Foundation (project number 22-19-00712, <https://rscf.ru/project/22-19-00712/>).

References

1. Diebold U. *Surface Science Reports* **48**, 53 (2003)
2. Fujishima A., Honda K. *Nature* **238**, 37 (1972)
3. Strukov D. B., Snider G. S., Stewart D. R., Williams R. S. *Nature* **453**, 80 (2008)
4. Dong R., Yan X., Zhang Z., Wang M. *Materials Research Bulletin* **61**, 101 (2015)

5. Breckenridge R. G., Hosler W. R. *Physical Review* **91**, 793 (1953)
6. Diebold U., Li M., Dulub O., Hebenstreit E. L. D., Hebenstreit W. *Surface Review and Letters* **07**, 613 (2000)
7. Aono M., Hasiguti R. R. *Physical Review B* **48**, 12406 (1993)
8. Yang S., Halliburton L. E., Manivannan A., Bunton P. H., Baker D. B., Klemm M., Horn S., Fujishima A. *Applied Physics Letters* **94**, 162114 (2009)
9. Brandão F. D., Pinheiro M. V. B., Ribeiro G. M., Medeiros-Ribeiro G., Krambrock K. *Physical Review B* **80**, 235204 (2009)
10. Brant A. T., Giles N. C., Sarker M. A. R., Watauchi S., Nagao M., Tanaka I., Tryk D. A., Manivannan A., Halliburton L. E. *Journal of Applied Physics* **114**, 113702 (2013)
11. Zhou S., Čížmár E., Potzger K., Krause M., Talut G., Helm M., Fassbender J., Zvyagin S. A., Wosnitza J., Schmidt H. *Physical Review B* **79**, 113201 (2009)
12. Ziegler J. F., Ziegler M., Biersack J. *Nuclear Instruments and Methods in Physics Research Section B: Beam Interactions with Materials and Atoms* **268**, 1818 (2010)
13. Stoll S., Schweiger A. *Journal of Magnetic Resonance* **178**, 42 (2006)
14. Al'tshuler S. A., Kozyrev B. M. *Electron Paramagnetic Resonance in Compounds of Transition Elements* (Wiley, New York, 1974)
15. Yoshimori A. *Journal of the Physical Society of Japan* **14**, 807 (1959)
16. Yang K., Dai Y., Huang B., Feng Y. P. *Physical Review B* **81**, 033202 (2010)